Journal of Sound and Vibration 329 (2010) 1780–1792

Contents lists available at ScienceDirect

Journal of Sound and Vibration

journal homepage: www.elsevier.com/locate/jsvi

Free vibration analysis of beams and rectangular plates with free edges by the discrete singular convolution

Xinwei Wang *, Suming Xu

MOE Key Lab of Structure Mechanics and Control for Aircraft, Institute of Structures & Strength, Nanjing University of Aeronautics and Astronautics, Nanjing 210016, China

ARTICLE INFO

Article history:
Received 12 August 2009
Received in revised form
18 November 2009
Accepted 6 December 2009
Handling Editor: L.G. Tham
Available online 30 December 2009

ABSTRACT

In this paper, free vibration of beams, annular plates, and rectangular plates with free boundaries are analyzed by using the discrete singular convolution (DSC). A novel method to apply the free boundary conditions is proposed. Detailed derivations are given. To validate the proposed method, eight examples, including the free vibrations of beams, annular plates and rectangular plates with free boundaries are analyzed. Two kernels, the regularized Shannon's kernel and the non-regularized Lagrange's delta sequence kernel, are tested. DSC results are compared with either analytical solutions or/and differential quadrature (DQ) data. It is demonstrated that the proposed method to incorporate the free boundary conditions is simple to use and can yield accurate frequency data for beams with a free end and plates with free edges. Thus, the proposed method for applying the boundary conditions extends the application range of the DSC.
© 2009 Elsevier Ltd. All rights reserved.

1. Introduction

Beams and plates are basic structural elements in engineering structures, thus are of great significance to aerospace, mechanical, and civil engineering. In 1973, Leissa [1] attempted to present comprehensive and accurate analytical results for the free vibration of beams and rectangular plate. Six cases exist for the beams and 21 cases exist for the rectangular plates, which involve the possible combinations of simply supported (S), clamped (C), and free (F) edge conditions. As analytical methods often fail or become too cumbersome to use, numerical simulation is one of the major approaches in engineering practice. Therefore, the analytical results [1] have been served as the references to validate various numerical methods.

More recently, the discrete singular convolution (DSC), proposed by Wei [2], has emerged as a local spectral method to combine the accuracy of global methods with the flexibility of local methods. The DSC has been shown a very promising approach for the vibration analysis of plates [3].

The discrete singular convolution proposed for the computer realization of singular convolutions [2,4]. The mathematical foundation of the DSC is the theory of distributions and the theory of wavelets. The DSC algorithm has been realized in both collocation and Galerkin formulations [5]. The method can handle complex geometry and boundary conditions in many applications, including the successful applications in solving some mechanical problems [6]. For example, the vibration and buckling of beams, the free vibration of Kirchhoff and Mindlin plates, the free vibration of conical and thick shallow shells under various combinations of boundary conditions [3,5,7–16], especially, the challenge problems of vibration analyses of plates with irregular internal supports [10] and vibrating at higher-order modes [13–15]. Recently, the applications of DSC were extended by

* Corresponding author.
E-mail address: wangx@nuaa.edu.cn (X. Wang).

0022-460X/$ - see front matter © 2009 Elsevier Ltd. All rights reserved.
doi:10.1016/j.jsv.2009.12.006

Civalek [17–19] to nonlinear analysis of thin rectangular plates on Winkler–Pasternak elastic foundations [17], free vibration of laminated composite conical and cylindrical shells [18], and three-dimensional vibration, buckling and bending analyses of thick rectangular plates [19]. More recently, the DSC together with mode superposition (MS) approaches successfully predicted the discrete high-frequency forced vibration of thin plates with either simply supported or clamped edges [20].

It is seen that methods of symmetric extension and anti-symmetric extension are successfully used for applying the clamped and simply supported boundary conditions in the DSC analysis. Very accurate results, including the high frequencies, are obtained for free vibration problems of thin rectangular plates with different combinations of simply supported, clamped and transversely supported with non-uniform elastic rotational restraint (E) edges [3]. Although methods of symmetric extension and anti-symmetric extension are simple and very effective to eliminate the fictitious points outside the solution domain; however, it cannot be used effectively for applying the free boundary conditions. Recently, the method of matched interface and boundary (MIB) was proposed by Wei and his co-workers [11,12] to overcome the difficulty of implementing free boundary conditions of beams and rectangular plates in the DSC algorithm. Accurate results are presented for the first 10 frequencies of the beams with free edges [11] and for the first five frequencies of the rectangular plates with free edges. Different combinations of M (the number of layers of fictitious values), L (the stencil width), and N (the number of grid points) are studied in the convergence analysis. Although the first 10 frequencies of the beams with free edges are very accurate; however, the accuracy of rectangular plates with free edges is not as high as that of rectangular plates without a free edges [3,12]. Besides, no information on the accuracy of the high-order frequencies is presented in [11,12].

It is also noticed that the method of matched interface and boundary (MIB) is not as simple as the methods of the symmetric extension and anti-symmetric extension. Therefore, the objective of the present work is to explore an alternative simple way for applying the free boundary conditions in the DSC algorithm. A simple way for treatment of the free boundary conditions is proposed. Formulations and solution procedures are worked out in detail. To validate the proposed method, eight examples, including the free vibration of beams with free ends, rectangular plates with a free edge, and challenging problems of annular plates with inner edge free and small ratios of inner radius to outer radius, and rectangular plates with all edges free, are analyzed by using the DSC. Two kernels, the regularized Shannon's kernel and the non-regularized Lagrange's delta sequence kernel, are tested. DSC results are compared with either analytical solutions or/and recalculated data by using the differential quadrature method (DQM) [21-22] or differential quadrature element method (DQEM) [23]. Some conclusions are drawn based on the results reported herein.

2. Theory

2.1. Free vibration of beams

For an Euler–Bernoulli beam with length L and cross-sectional area A, the governing differential equation for free vibration is given by

$$EI\frac{\mathrm{d}^4w(x)}{\mathrm{d}x^4}=\rho A\omega^2w(x) \tag{1}$$

where E and I are modulus of elasticity and the second moment area about the neutral axis, $w(x)$ is the deflection of the beam, x is the Cartesian coordinate in the neutral axis of the beam, ρ is the mass density of the beam, and ω is the circular frequency, respectively.

The boundary conditions are

(1) Clamped end (C):

$$w=\frac{\mathrm{d}w}{\mathrm{d}x}=0 \tag{2a,b}$$

(2) Simply supported end (S):

$$w=\frac{\mathrm{d}^2w}{\mathrm{d}x^2}=0 \tag{3a,b}$$

(3) Free end (F):

$$\frac{\mathrm{d}^2w}{\mathrm{d}x^2}=\frac{\mathrm{d}^3w}{\mathrm{d}x^3}=0 \tag{4a,b}$$

2.2. Free vibration of rectangular plates

For an isotropic rectangular Kirchhoff plate with length a, width b and thickness t, the governing differential equation for free vibration is given by

$$\frac{\partial^4w(x,y)}{\partial x^4}+2\frac{\partial^4w(x,y)}{\partial x^2\partial y^2}+\frac{\partial^4w(x,y)}{\partial y^4}=\frac{\rho t\omega^2w(x,y)}{D} \tag{5}$$

where x and y are the Cartesian coordinates in the middle plane of the plate, $w(x,y)$ is the deflection of the plate, ρ is the mass density, $D=Et^3/[12(1-\nu^2)]$ is the flexural rigidity of the plate, E and ν are the modulus of elasticity and Poisson's ratio, and ω is the circular frequency, respectively.

The boundary conditions are

(1) Clamped edge (C):

$$w=\frac{\partial w}{\partial x}=0 \quad (x=0 \text{ or } a), \tag{6a,b}$$

$$w=\frac{\partial w}{\partial y}=0 \quad (y=0 \text{ or } b) \tag{7a,b}$$

(2) Simply-supported edge (S):

$$w=\frac{\partial^2 w}{\partial x^2}+\nu\frac{\partial^2 w}{\partial y^2}=0 \ \ (x=0 \text{ or } a) \tag{8a,b}$$

$$w=\frac{\partial^2 w}{\partial y^2}+\nu\frac{\partial^2 w}{\partial x^2}=0 \ \ (y=0 \text{ or } b) \tag{9a,b}$$

(3) Free edge (F):

$$\frac{\partial^2 w}{\partial x^2}+\nu\frac{\partial^2 w}{\partial y^2}=\frac{\partial^3 w}{\partial x^3}+(2-\nu)\frac{\partial^3 w}{\partial x\partial y^2}=0 \quad (x=0 \text{ or } a) \tag{10a,b}$$

$$\frac{\partial^2 w}{\partial y^2}+\nu\frac{\partial^2 w}{\partial x^2}=\frac{\partial^3 w}{\partial y^3}+(2-\nu)\frac{\partial^3 w}{\partial y\partial x^2}=0 \ \ (y=0 \text{ or } b) \tag{11a,b}$$

2.3. Free vibration of annular plates

For an isotropic annular plate with inner radius b, outer radius a, and thickness t, the governing differential equation for axi-symmetric free vibration is given by

$$\frac{\mathrm{d}^4 w(r)}{\mathrm{d}r^4}+\frac{2}{r}\frac{\mathrm{d}^3 w(r)}{\mathrm{d}r^3}-\frac{1}{r^2}\frac{\mathrm{d}^2 w(r)}{\mathrm{d}r^2}+\frac{1}{r^3}\frac{\mathrm{d}w(r)}{\mathrm{d}r}=\frac{\rho t\omega^2}{D}w(r) \tag{12}$$

where r is the polar coordinate in the middle plane of the plate, $w(r)$ is the deflection of the plate, ρ is the mass density, $D=Et^3/[12(1-\nu^2)]$ is the flexural rigidity of the plate, E and ν are the modulus of elasticity and Poisson's ratio, and ω is the circular frequency, respectively.

The boundary conditions are

(1) Clamped edge (C):

$$w(r)=\frac{\mathrm{d}w(r)}{\mathrm{d}r}=0 \ \ (r=b \text{ or } a) \tag{13a,b}$$

(2) Simply supported edge (S):

$$w(r)=\frac{\mathrm{d}^2 w(r)}{\mathrm{d}r^2}+\frac{\nu}{r}\frac{\mathrm{d}w(r)}{\mathrm{d}r}=0 \ \ (r=b \text{ or } a) \tag{14a,b}$$

(3) Free edge (F):

$$\left(\frac{\mathrm{d}^2 w}{\mathrm{d}r^2}+\nu\frac{1}{r}\frac{\mathrm{d}w}{\mathrm{d}r}\right)=\left(\frac{\mathrm{d}^3 w}{\mathrm{d}r^3}+\frac{1}{r}\frac{\mathrm{d}^2 w}{\mathrm{d}r^2}-\frac{1}{r^2}\frac{\mathrm{d}w}{\mathrm{d}r}\right)=0 \ \ (r=b \text{ or } a) \tag{15a,b}$$

3. DSC and the solution procedures

The discrete singular convolution (DSC) is employed herein for free vibration analysis. In the DSC, a function $w(x)$ and its jth order derivative with respect to x are approximated via a discretized convolution, namely [5],

$$w^{(j)}(x)\approx\sum_{k=-M}^{M}\delta_{\sigma,\Delta}^{(j)}(x-x_k)w(x_k) \ \ (j=0,1,2,\ldots) \tag{16}$$

where $2M+1$ is the computational bandwidth, $x_k (k=-M,-M+1,\ldots,-1,0,1,\ldots,M-1,M)$ are uniformly distributed grid points, and $\delta^{(j)}_{\sigma,\Delta}(x-x_k)$ is a collective symbol for the delta kernels of Dirichlet type and is given by

$$\delta^{(j)}_{\alpha,\delta}(x-x_k)=\left(\frac{\mathrm{d}}{\mathrm{d}x}\right)^j \delta_{\alpha,\delta}(x-x_k) \tag{17}$$

Although there are many DSC kernels available, two kernels are adopted in the present study, namely, the non-regularized Lagrange's delta sequence kernel (DSC-LK [3,5]) and the regularized Shannon's kernel (DSC-RSK) [5]. The non-regularized Lagrange's delta sequence kernel, already discretized, is given by

$$\delta_{M,k}(x-x_k)=\begin{cases} L_{M,k}(x-x_k) & \text{for} -\beta\le x\le\beta \\ 0 & \text{otherwise}\end{cases} \quad \text{for } M=1,2,\ldots \tag{18}$$

where $\beta\le L_c$ (L_c is the length of beam, plate length or plate width), and $L_{M,k}(x)$ is the Lagrange interpolation defined by [3]

$$L_{M,k}(x)=\prod_{i=k-M,i\neq k}^{k+M}\frac{x-x_i}{x_k-x_i}(M\ge 1) \tag{19}$$

The regularized Shannon's delta kernel is discretized by [5]

$$\delta_{\Delta,\delta}(x-x_k)=\frac{\sin[\pi(x-x_k)/\Delta]}{\pi(x-x_k)/\Delta}\,e^{-(x-x_k)^2/2\sigma^2} \tag{20}$$

where $\Delta=L_c/(N-1)$ is the grid spacing and N ($N\ge M+1$) the number of grid points.

The higher-order differentiation matrix elements, $\delta^{(j)}_{\alpha,\delta}(x_m-x_k)$, can be computed by

$$\delta^{(j)}_{\alpha,\delta}(x_m-x_k)=\left[\left(\frac{\mathrm{d}}{\mathrm{d}x}\right)^j \delta_{\alpha,\delta}(x-x_k)\right]_{x=x_m} \tag{21}$$

Thus, one has

$$w'(0)=w^{(1)}(0)\approx\sum_{k=-M}^{M}\delta^{(1)}_{\sigma,\Delta}(x-x_k)w(x_k)=\sum_{k=-M}^{M}A_{0k}w(x_k)=\sum_{k=-M}^{M}A_{0k}w_k \tag{22}$$

$$w''(0)=w^{(2)}(0)\approx\sum_{k=-M}^{M}\delta^{(2)}_{\sigma,\Delta}(x-x_k)w(x_k)=\sum_{k=-M}^{M}B_{0k}w(x_k)=\sum_{k=-M}^{M}B_{0k}w_k \tag{23}$$

$$w'''(0)=w^{(3)}(0)\approx\sum_{k=-M}^{M}\delta^{(3)}_{\sigma,\Delta}(x-x_k)w(x_k)=\sum_{k=-M}^{M}C_{0k}w(x_k)=\sum_{k=-M}^{M}C_{0k}w_k \tag{24}$$

$$w^{\mathrm{IV}}(0)=w^{(4)}(0)\approx\sum_{k=-M}^{M}\delta^{(4)}_{\sigma,\Delta}(x-x_k)w(x_k)=\sum_{k=-M}^{M}D_{0k}w(x_k)=\sum_{k=-M}^{M}D_{0k}w_k \tag{25}$$

where the differentiation matrix elements, $A_{0k}, B_{0k}, C_{0k}, D_{0k}$, are called here the "weighting coefficients" of the first-, second-, third- and fourth-order derivatives with respect to x, since they are exactly the corresponding weighting coefficients at the middle point in the DQM if the non-regularized Lagrange's delta sequence kernel is used. It was shown earlier that the error of the DQM at the center point is the smallest with uniform grid spacing as compared with various non-uniform grid spacing [21].

A complete numerical algorithm has to provide a scheme for handling various boundary conditions to eliminate fictitious points. The Dirichlet boundary condition, $w=0$, can be easily specified at the boundary. For beams, Eqs. (2b) and (3b) can be applied by the method of symmetric or anti-symmetric extensions, respectively [3,5,6]. To apply the free boundary conditions, a more general form based on the symmetric extension method with a slight modification is proposed herein. Without loss of generality, using Taylor's series expansion for $w(x)$ and $w(-x)$ at $x_0=0$ and retaining the terms up to x^3 yields

$$w(-x)=w(x)+w'(0)(-2x)+w'''(0)(-x^3/3) \tag{26}$$

where $x\in[-\beta,\beta](\beta\le L_c)$. In general, $x_0\neq 0$. In such a case, just simply replace x in Eq. (26) by $x-x_0$. Eq. (26) is to be used to eliminate the fictitious points outside the solution domain with free boundaries.

For illustration, consider first the free boundary condition of a beam at its left end ($x=0$). Since $A_{0(-k)}=-A_{0k}, B_{0(-k)}=B_{0k}, C_{0(-k)}=-C_{0k}, D_{0(-k)}=D_{0k}, (k=1,2,\ldots,M)$, thus, it is easy to show by substituting Eq. (26) into Eqs. (22)–(25) that

$$w'(0)=w'_0=\sum_{k=-M}^{M}A_{0k}w_k=w'_0 \tag{27}$$

$$w''(0)=w_0''=\sum_{k=-M}^{M}B_{0k}w_k=\sum_{k=0}^{M}B_kw_k+w_0'\sum_{k=1}^{M}B_{0k}(-2x_k)+w_0'''\sum_{k=1}^{M}B_{0k}(-x_k^3/3)=\sum_{k=0}^{M}B_kw_k+B_{M+1}w_0'+B_{M+2}w_0''' \tag{28}$$

$$w'''(0)=w_0'''=\sum_{k=-M}^{M}C_{0k}w_k=w_0''' \tag{29}$$

$$w^{\mathrm{IV}}(0)=w_0^{\mathrm{IV}}=\sum_{k=-M}^{M}D_{0k}w_k=\sum_{k=0}^{M}D_kw_k+w_0'\sum_{k=1}^{M}D_{0k}(-2x_k)+w_0'''\sum_{k=1}^{M}D_{0k}(-x_k^3/3)=\sum_{k=0}^{M}D_kw_k+D_{M+1}w_0'+D_{M+2}w_0''' \tag{30}$$

where $B_0=B_{00}$, $B_k=2B_{0k}(k=1,2,\ldots,M)$, $B_{M+1}=-\sum_{k=1}^{M}2B_{0k}x_k$, $B_{M+2}=-\sum_{k=1}^{M}B_{0k}x_k^3/3$, $D_0=D_{00}$, $D_k=2D_{0k}$ $(k=1,2,\ldots,M)$, $D_{M+1}=-\sum_{k=1}^{M}2D_{0k}x_k$, $D_{M+2}=-\sum_{k=1}^{M}D_{0k}x_k^3/3$, respectively.

Since $w'''(0)=0$ at the free end, Eq. (26) is further reduced to

$$w(-x)=w(x)+w'(0)(-2x) \tag{31}$$

Eq. (31) is exactly the same expression as was proposed earlier by present authors [24]. Thus, equation $w''(0)=0$ is used to eliminate the remaining additional degree of freedom at the boundary point, i.e., w_0'. Applying $w''(0)=0$ and using Eq. (28) together with $w'''(0)=0$ yield

$$w_0'=-\sum_{k=0}^{M}(B_k/B_{M+1})w_k \tag{32}$$

For simplicity, assume the total number of the grid points N equals to $M+1$. After applying the boundary conditions, the governing differential equation for free vibration of F–C or F–S beams in terms of DSC is

$$\sum_{j=0}^{M-1}\overline{D}_{ij}w_j=\frac{\rho A\omega^2w_i}{EI}\quad(i=0,1,2,\ldots,M-1) \tag{33}$$

where the over-bar means that the corresponding coefficients have been modified by eliminating all fictitious points and additional degrees of freedom. For example, $\overline{D}_{ij}=D_{ij}-D_{i(M+1)}B_i/B_{M+1}$ for the F–C beam.

Solving Eq. (33) by a standard eigenvalue solver yields the frequencies of the beam.

Consider next the free boundary condition of annular plates at inner boundary ($r=b$). Since $x_0\neq0$, then $x=r-b$ should be used in Eq. (26). For convenience, Eq. (15b) can be re-written to the following equivalent form by considering Eq. (15a),

$$\left(\frac{\mathrm{d}^2w}{\mathrm{d}r^2}+\frac{rv}{1+v}\frac{\mathrm{d}^3w}{\mathrm{d}r^3}\right)_{r=b}=0 \tag{34}$$

Substituting Eqs. (27)–(29) into Eqs. (15a) and (34) results

$$\left(\frac{v}{b}+B_{M+1}\right)w_0'+B_{M+2}w_0'''=-\sum_{k=0}^{M}B_kw_k \tag{35}$$

$$B_{M+1}w_0'+\left(\frac{vb}{1+v}+B_{M+2}\right)w_0'''=-\sum_{k=0}^{M}B_kw_k \tag{36}$$

Solving Eqs. (35) and (36) simultaneously yields

$$\begin{cases}w_0'=\left(-\dfrac{vb}{1+v}\right)/\left\{\left(\dfrac{vb}{1+v}+B_{M+2}\right)\left(\dfrac{v}{b}+B_{M+1}\right)-B_{M+1}B_{M+2}\right\}\displaystyle\sum_{k=0}^{M}B_kw_k\\ w_0'''=\left(-\dfrac{v}{b}\right)/\left\{\left(\dfrac{vb}{1+v}+B_{M+2}\right)\left(\dfrac{v}{b}+B_{M+1}\right)-B_{M+1}B_{M+2}\right\}\displaystyle\sum_{k=0}^{M}B_kw_k\end{cases} \tag{37}$$

For annular plates, one of the clamped boundary conditions, Eq. (13b), can be applied by the method of symmetric extension [3,5,6]. To apply one of the simply supported boundary conditions at $r=a$, Eq. (14b), Eq. (31) is used. One has

$$\left(\frac{v}{a}+B_{M+1}\right)w_M'=-\sum_{k=0}^{M}B_kw_k \tag{38}$$

It should be mentioned that one should replace x with $x=r-a$ in Eq. (31), since $x_0=a$. Solving Eq. (38) yields

$$w_M'=-1/\left(\frac{v}{a}+B_{M+1}\right)\sum_{k=0}^{M}B_kw_k \tag{39}$$

After applying the boundary conditions, the governing differential equation for free vibration of F–C and F–S annular plates in terms of DSC is

$$\sum_{j=0}^{M-1}\overline{D}_{ij}w_j+\frac{2}{r_i}\sum_{j=0}^{M-1}\overline{C}_{ij}w_j-\frac{1}{r_i^2}\sum_{j=0}^{M-1}\overline{B}_{ij}w_j+\frac{1}{r_i^3}\sum_{j=0}^{M-1}\overline{A}_{ij}w_j=\frac{\rho t\omega^2 w_i}{D}\quad(i=0,1,2,\ldots,M-1) \tag{40}$$

where the over-bar means that the corresponding coefficients have been modified to eliminate all fictitious points and additional degrees of freedom.

Solving Eq. (40) by a standard eigenvalue solver yields the frequencies of the annular plates.

Consider last the rectangular plates. The method of symmetric extension [3,5,6] is used for the clamped edges and the method of anti-symmetric extension [3,5,6] is used for the simply supported edges. For the free boundary, Eq. (26) is used to eliminate all degrees of freedom at fictitious points. Consider both ends free. After eliminating all degrees of freedom at fictitious points, following general expressions can be obtained, namely,

$$w'(x_i)=w_i'\approx\sum_{k=0}^{M}A_{ik}w_k+A_{i(M+1)}w_0'+A_{i(M+2)}w_0'''+A_{i(M+3)}w_M'+A_{i(M+4)}w_M'''=\sum_{k=0}^{M+4}A_{ik}\overline{w}_k \tag{41}$$

$$w''(x_i)=w_i''\approx\sum_{k=0}^{M}B_{ik}w_k+B_{i(M+1)}w_0'+B_{i(M+2)}w_0'''+B_{i(M+3)}w_M'+B_{i(M+4)}w_M'''=\sum_{k=0}^{M+4}B_{ik}\overline{w}_k \tag{42}$$

$$w'''(x_i)=w_i'''\approx\sum_{k=0}^{M}C_{ik}w_k+C_{i(M+1)}w_0'+C_{i(M+2)}w_0'''+C_{i(M+3)}w_M'+C_{i(M+4)}w_M'''=\sum_{k=0}^{M+4}C_{ik}\overline{w}_k \tag{43}$$

$$w^{\mathrm{IV}}(x_i)=w_i^{\mathrm{IV}}\approx\sum_{k=0}^{M}D_{ik}w_k+D_{i(M+1)}w_0'+D_{i(M+2)}w_0'''+D_{i(M+3)}w_M'+D_{i(M+4)}w_M'''=\sum_{k=0}^{M+4}D_{ik}\overline{w}_k\quad(i=0,1,\ldots,M) \tag{44}$$

It seems at first that the programming might be complicated since boundary points have three degrees of freedom while all inner grid points have only one degree of freedom. A relative simple way can alleviate this difficulty. Let N_x, N_y be the total number of grid points in the x and y directions, schematically shown in Fig. 1. Note that $M=N_x-1$ or N_y-1. For simplifying the programming, $4N_x+4N_y$ more grid points, denoted by shaded circles in Fig. 1 and with one degree of freedom (either w_x', or w_x''', or w_y' or w_y''') each, are introduced. Since each grid point has one degree of freedom, namely, w for the $N_x\times N_y$ grid points located on the plate, w_x' for the first $2N_y$ additional grid points close to the right-hand side, w_x''' for the remaining $2N_y$ additional grid points on the right-hand side, w_y' for the $2N_x$ additional grid points on the top of the plate close to the edge, and w_y''' for the remaining $2N_x$ additional grid points on the top of the plate, thus the programming in two dimensions is still not difficult. It should be pointed out that the location of the additional points is unimportant.

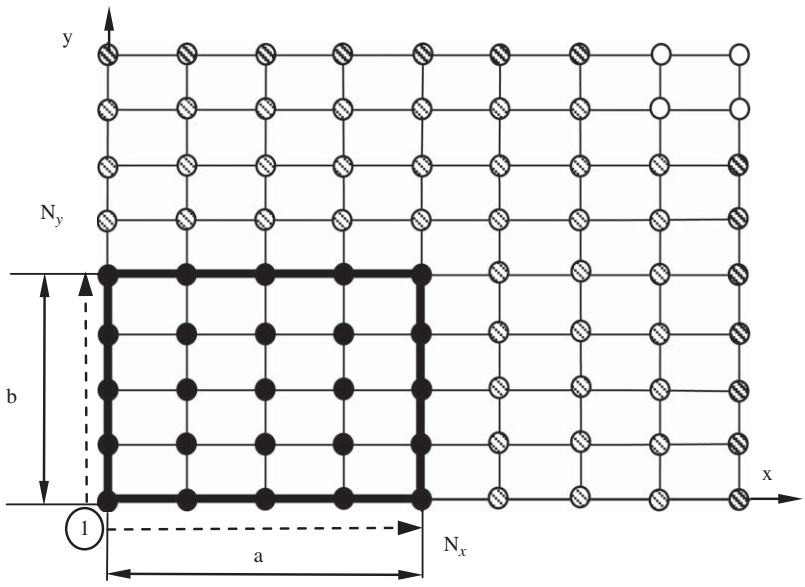

Fig. 1. Sketch of a rectangular plate with uniform grid points ($M+1=N_x=N_y=5$).

In terms of the DSC, the governing differential equation for free vibration at all grid points can be expressed as

$$\sum_{k=0}^{M+4} D_{ik}^{x}\overline{w}_{kl}+2\sum_{j=0}^{M+4}\sum_{k=0}^{M+4} B_{ij}^{x}B_{lk}^{y}\overline{w}_{jk}+\sum_{k=0}^{M+4} D_{lk}^{y}\overline{w}_{ik}=\frac{\rho t\omega^2 w_{il}}{D}\quad (i=0,1,2,\ldots,M,\quad l=0,1,2,\ldots,M) \tag{45}$$

where $D_{ij}^{x}, D_{ij}^{y}, B_{ij}^{x}, B_{ij}^{y}$ $(i=0,1,\ldots,M, j=0,1,\ldots,M,M+1,M+2)$ are the "weighting coefficients" of the fourth-order derivatives with respect to x or y, and the "weighting coefficients" of the second-order derivatives with respect to x or y, calculated by using Eqs. (44) and (42) with $N_x=N_y=M+1$; $\overline{w}_{ij}$ are either values of the deflection w at grid point $ij(i=0,1,\ldots,M; j=0,1,\ldots,M)$, or its first derivative with respective to x or y at the boundary grid point $ij(i=M+1,M+2; j=M+1,M+2)$, or its third derivative with respective to x or y at the boundary grid point $ij(i=M+3,M+4; j=M+3,M+4)$, respectively.

It should be mentioned that only equations at inner grid points are necessary if all four edges are the combinations of clamped (C) or/and simply supported (S) boundary conditions. For rectangular plate with all edge clamped (CCCC), for example, Eq. (45) can be re-written by

$$\sum_{k=1}^{M-1} D_{ik}^{x}\overline{w}_{kl}+2\sum_{j=1}^{M-1}\sum_{k=1}^{M-1} B_{ij}^{x}B_{lk}^{y}\overline{w}_{jk}+\sum_{k=1}^{M-1} D_{lk}^{y}\overline{w}_{ik}=\frac{\rho t\omega^2 w_{il}}{D}\quad (i=1,2,\ldots,M-1;\quad l=1,2,\ldots,M-1) \tag{46}$$

If one free boundary is involved, e.g., CFCC plate (free at edge of $y=0$), then Eq. (11) is used to eliminate the non-zero w_y' and w_y''' at the boundary points. In terms of the DSC, Eq. (11) at $y=0$ becomes,

$$\begin{cases} \displaystyle\sum_{k=0,k\neq M}^{M+2} B_{0k}^{y}\overline{w}_{ik}+\nu\sum_{k=1}^{M-1} B_{ik}^{x}w_{k0}=0 \quad (i=1,2,\ldots,M-1) \\ \displaystyle\sum_{k=0,k\neq M}^{M+2} C_{0k}^{y}\overline{w}_{ik}+(2-\nu)\sum_{j=1}^{M-1}\sum_{k=0,k\neq M}^{M+2} B_{ij}^{x}A_{0k}^{y}\overline{w}_{jk}=0 \end{cases} \tag{47}$$

For FFFF plates, Eqs. (10) and (11) can be expressed in a similar form of Eq. (47) at all four edges. After applying the boundary conditions and eliminating the non-zero derivatives by using Eq. (47), Eq. (45) or Eq. (46) can be re-written in the matrix form

$$[K]\{w\}=\overline{\lambda}\{w\} \tag{48}$$

Eq. (48) is a standard eigenvalue problem. Frequencies can be obtained by utilizing a standard eigensolver.

4. Results and discussions

For comparison purpose, frequency parameters are introduced. For beams, the frequency parameter Ω is defined by $\Omega=\omega L^2\sqrt{\rho A/EI}$. For annular plates, the frequency parameter Ω is defined by $\Omega=\omega a^2\sqrt{\rho t/D}$. For rectangular plates, the frequency parameter λ is defined by $\lambda=\omega a^2\sqrt{\rho/D}$.

The DSC with the proposed method for free boundary conditions is used to obtain the solutions of beams, annular plates, and rectangular plates with free boundaries. Computer programs are written and eight examples are studied. Results obtained by the DQM and existing data are also used for the comparisons.

Consider first the free vibration of Euler–Bernoulli beams with one or two free ends. Three combinations of boundary conditions, namely, F–C, F–S and F–F, are investigated. Tables 1– 3 lists the first six frequency parameters by the DSC-LK with uniform grid spacing and DQM with non-uniform grid spacing, together with the exact solutions by Leissa [1]. It is seen that the accuracy of the solutions by DSC-LK is good. As is expected the DQM with $M=49$ yields exactly the same results as the exact solutions. Figs. 2 and 3 show the percentage relative error of all frequency parameters obtained by the DSC-LK and DSC-RSK, where the percentage relative error is defined by

$$\text{Relative error}(\%)=(\Omega_{\text{DSC}}-\Omega_{\text{exact}})/\Omega_{\text{exact}}\times 100\% \tag{49}$$

From Figs. 2 and 3, it is seen that the percentage relative error is less than 1 up to first 40 modes for $M=49$, the maximum percent relative error is less than 10 by the DSC-LK and 4 by the DSC-RK for all modes. For lower frequencies, there is no difference between data by DSC-LK and by DSC-RSK. For high frequencies, the DSC-RSK yields more accurate results than the DSC-LK.

Table 1
Frequency parameter Ω for F-C beam (M=49).

Mode No	1	2	3	4	5	6
Leissa [1]	3.5160	22.034	61.697	120.902	199.860	298.556
DSC-LK	3.5157	22.027	61.665	120.815	199.677	298.229
DSC-RSK	3.5157	22.027	61.665	120.815	199.678	298.230
DQM	3.5160	22.034	61.697	120.902	199.860	298.556

Table 2
Frequency parameter Ω for F-S beam (M=49).

Mode No	1	2	3	4	5	6
Leissa [1]	15.418	49.965	104.248	178.270	272.031	385.531
DSC-LK	15.414	49.941	104.176	178.112	271.737	385.042
DSC-RSK	15.414	49.941	104.176	178.112	271.738	385.043
DQM	15.418	49.965	104.248	178.270	272.031	385.531

Table 3
Frequency parameter Ω for F-F beam (M=49).

Mode No	1	2	3	4	5	6
Leissa [1]	22.373	61.673	120.903	199.859	298.556	416.991
DSC-LK	22.359	61.607	120.726	199.487	297.883	415.894
DSC-RSK	22.359	61.607	120.726	199.487	297.885	415.897
DQM	22.373	61.673	120.903	199.859	298.556	416.991

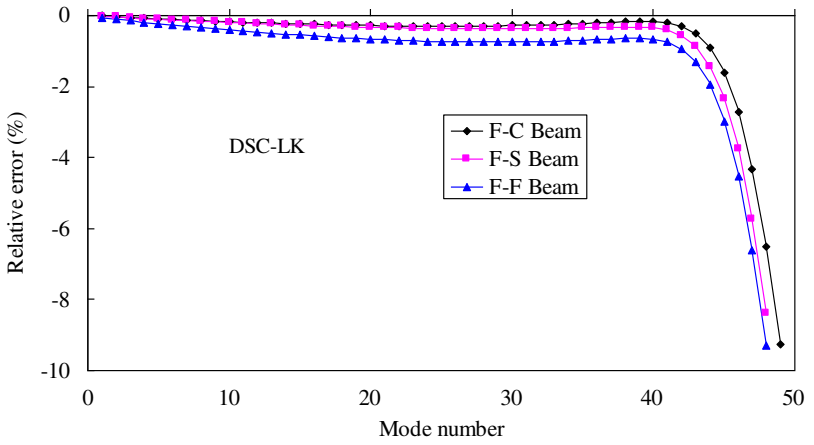

Fig. 2. Percentage relative errors of the DSC-LK results for beams of F–C, F–S and F–F (M=49).

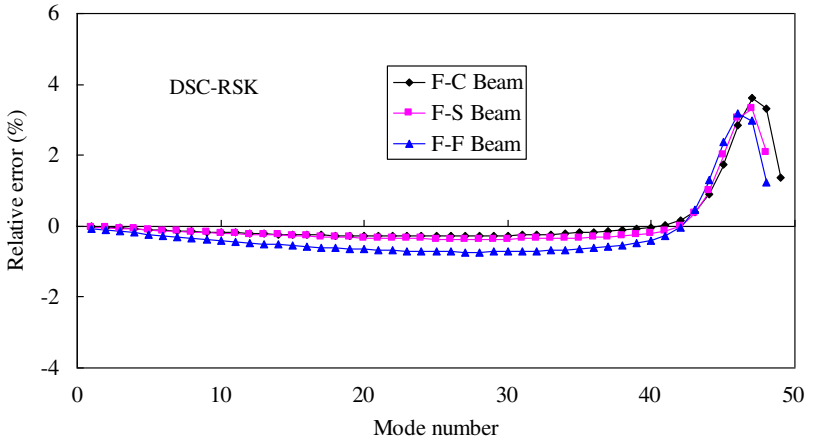

Fig. 3. Percentage relative errors of the DSC-RSK results for beams of F–C, F–S and F–F (M=49).

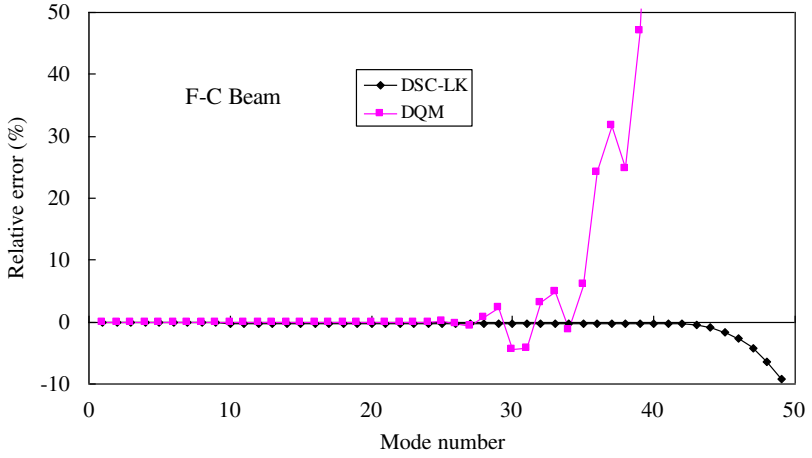

Fig. 4. Comparisons of the percentage relative errors of the DSC results with DQM results for F–C beam (M=49).

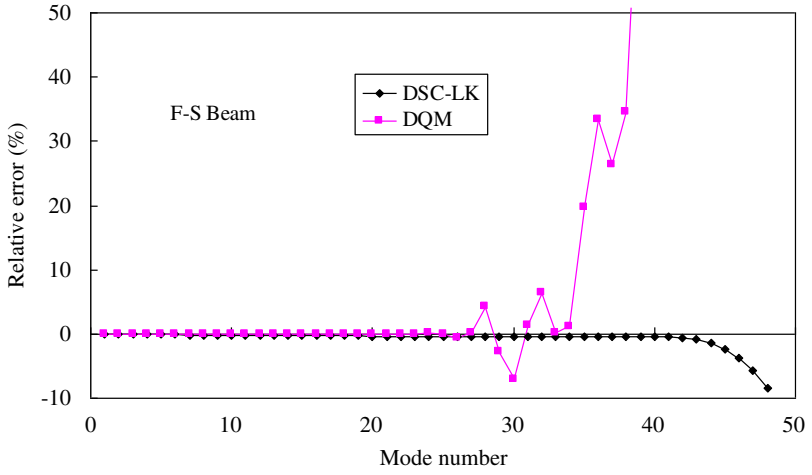

Fig. 5. Comparisons of the percentage relative errors of the DSC results with DQM results for F–S beam (M=49).

Figs. 4 and 5 show the comparisons of the percentage relative error of DSC-LK data with DQM results for the F–C beam and F–S beam, respectively. The following non-uniform grids are used for obtaining results by the DQM,

$$x_i = L(1-\cos[i\pi/M])/2 \quad (i=0,1,\ldots,M) \tag{50}$$

It is seen that the percentage relative error of DQM results are small up to first 25 modes, but very large for the much higher modes. It should be pointed out that for the first 25 modes, the percentage relative error of DQM results is smaller as compared with that of DSC results, also clearly seen from Tables 1 and Table 2. This is expected since approximation is introduced in the DSC, namely, in Eq. (26) or Eq. (31), for the treatment of the free boundary conditions. It may be concluded that the proposed method for applying the free boundary is simple and convenient to use. The overall behavior of the DSC seems retained, but the accuracy of the DSC results is not as high as in the cases of beams without a free boundary.

Consider next the free vibration of isotropic annular plates with inner edge free and outer edge clamped or simply supported. Relative small ratios of inner radius to outer radius, i.e., $b/a=0.1$ and 0.3, are considered, since it is difficult to obtain very accurate fundamental frequencies numerically for such cases. The following uniform grid spacing is used for the DSC, namely,

$$r_i = b+i\Delta r \quad (i=0,1,2,\ldots,M) \tag{51}$$

where $\Delta r=(a-b)/M$.

Tables 4 and 5 list the fundamental frequency parameters by the DSC-LK, together with the analytical solutions by Leissa [25] and existing data by the optimized Rayleigh–Ritz method(ORRM) [26,27] and by the DQM [28,29]. It is seen that relatively accurate results are obtained by the DSC for the first time. The larger the b/a, the more accuracy of the DSC results.

Table 4
Fundamental frequency parameter Ω for Annular plates (M=49, b/a=0.1, ν=1/3).

	Leissa [25]	ORRM [26]	ORRM [27]	DQM [28]	DQM [29]	DSC-LK
F-C	10.15	10.13	9.996	13.41	10.13	9.78
F-S	4.86	4.890	4.857	7.138	4.890	4.611

Table 5
Fundamental frequency parameter Ω for Annular plates (M=49, b/a=0.3, ν=1/3).

	Leissa [25]	ORRM [26]	ORRM [27]	DQM [28]	DQM [29]	DSC-LK
F-C	11.37	11.34	11.33	11.31	11.34	11.32
F-S	4.654	4.659	4.619	4.633	4.659	4.653

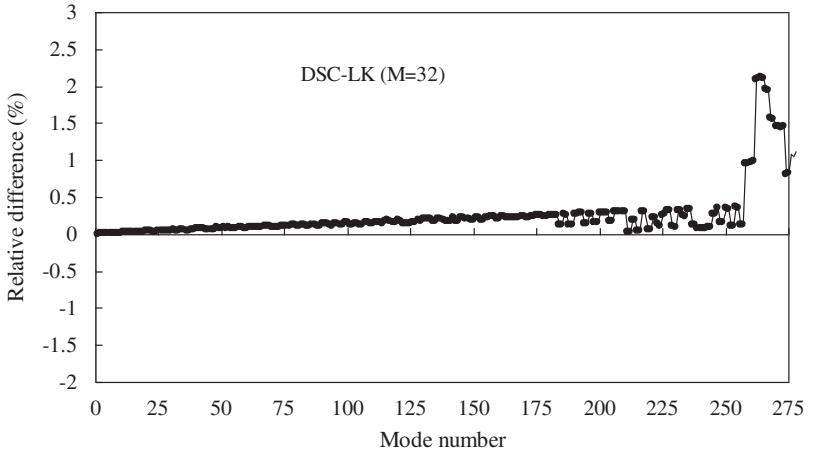

Fig. 6. The percentage relative difference of the DSC results with DQM results for CCCC rectangular plate (M=32).

Consider last the free vibration of isotropic rectangular Kirchhoff plates. Three combinations of boundary conditions, i.e., CCCC, CFCC, and FFFF, are investigated. For clamped boundary condition, the method of symmetric extension [3] is used, for the free boundary, the proposed method is used. $N_x = N_y = M+1 (M = 32)$ are used in the analysis. Except for the FFFF rectangular plate, the aspect ratio $a/b = 1$ is considered for illustrations. The following uniform grid spacing is used for the DSC, namely,

$$x_i = i\,\Delta a, \quad y_i = i\,\Delta b \ \ (i = 0, 1, 2, \ldots, M) \tag{52}$$

where $\Delta a = a/M$, $\Delta b = b/M$.

For comparisons, the problems are also analyzed by the DQM or the new version of differential quadrature element method (DQEM) [30]. For obtaining reliable solutions by the DQM or the DQEM, following non-uniform grid points are used:

$$x_i = a(1-\cos[i\pi/M])/2$$

$$y_i = b(1-\cos[i\pi/M])/2, \quad (i = 0, 1, \ldots, M) \tag{53}$$

Figs. 6–8 show the comparisons of the percentage relative difference of DSC-LK data with results by using the DQM or DQEM for the CCCC, CFCC and FFFF rectangular plates, respectively. The percentage relative difference is defined by

$$\text{Relative difference}(\%) = (\Omega_{\text{DSC}} - \Omega_{\text{DQM}})/\Omega_{\text{DQM}} \times 100\% \tag{54}$$

It is seen that the percentage relative difference with results of the DQM (or DQEM) are small up to first 275 modes for CCCC and CFCC plates. Fig. 8 shows only the difference up to the first 200 modes for the FFFF plate, since DQEM may yield complex eigenvalues starting from the 245 mode. For DSC with proposed method to treat the free boundary conditions, all eigenvalues are real number. It is observed from Fig. 8 and Table 8 that there is no much difference for the two kernels for the lower order frequencies. Thus only the DSC-LK data are presented in Tables 6, 7 and 9. It is also observed that for CFCC and FFFF plates, percentage relative difference is slightly larger than the CCCC plate. It is also seen from Tables 1 to 9 that the accuracy of the DSC results for the plates is a little lower than that for the beams. In Tables 7 and 8, results obtained by DSC with the matched interface and boundary (MIB) method [12] are also cited for comparisons. DSC-1 corresponds the

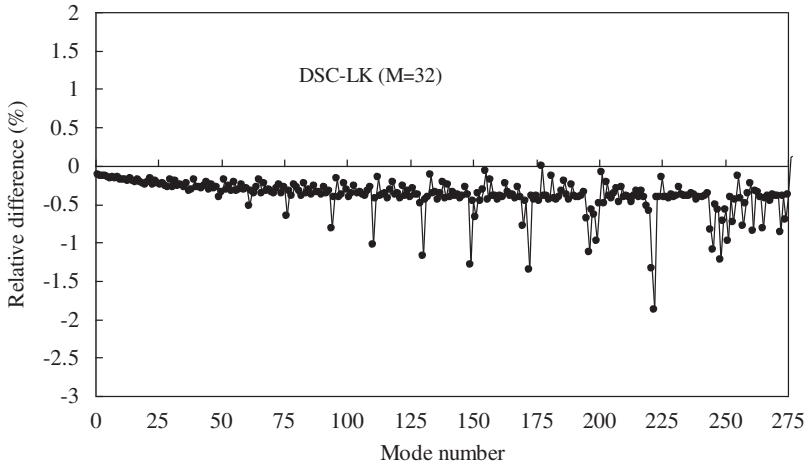

Fig. 7. The percentage relative difference of the DSC results with DQM results for CFCC rectangular plate (M=32).

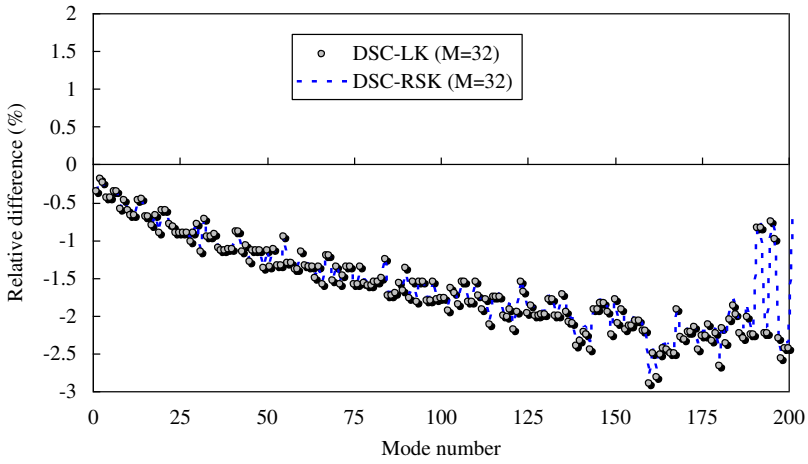

Fig. 8. The percentage relative difference of the DSC results with DQEM results for FFFF rectangular plate (M=32).

Table 6
Frequency parameter λ for CCCC plate (a/b=1).

Mode No	1	2	3	4	5	6
Leissa [1]	35.992	73.413	73.413	108.27	131.64	132.24
DSC-LK	35.986	73.399	73.399	108.23	131.57	132.22
DQM	35.985	73.394	73.394	108.22	131.58	132.20

Table 7
Frequency parameter λ for CFCC plate (a/b=1, ν=0.3).

Mode No	1	2	3	4	5	6
Leissa [1]	24.020	40.039	63.493	76.761	80.713	116.80
DSC-LK	23.888	39.942	63.131	76.601	80.447	116.46
DSC-1 [12]	23.985	40.194	63.454	76.913	80.967	N/A
DSC-2 [12]	24.157	40.547	62.517	76.161	81.095	N/A
DQM	23.918	39.995	63.216	76.708	80.566	116.65

adaptive grid ($M=4$,$N=17$), DSC-2 corresponds $M=2$ and $N=13$. Only 5 frequency parameters are reported in [12] and no information on the high-order frequency. It should be pointed out that the results of lower modes by using the new version of differential quadrature element method (DQEM) [30] are generally more accurate than the analytical data by

Table 8
Frequency parameter λ for FFFF plate (a/b=1, ν=0.3).

Mode No	1	2	3	4	5	6
Leissa [1]	13.489	19.789	24.432	35.024	35.024	61.526
DSC-RSK	13.420	19.559	24.213	34.649	34.649	60.880
DSC-LK	13.419	19.559	24.212	34.646	34.646	60.878
DSC-1 [12]	13.505	19.597	24.335	34.361	34.943	N/A
DSC-2 [12]	13.080	19.595	24.119	34.547	36.270	N/A
DQEM [30]	13.468	19.596	24.270	34.802	34.802	61.257

Table 9
Frequency parameter λ for FFFF plate (ν=0.3).

Mode sequence	a/b	2/5	2/3	1	3/2	5/2
1	Leissa [1]	3.4629	8.9459	13.489	20.128	21.643
	DSC-LK	3.4268	8.8934	13.419	20.010	21.418
	DQEM	3.4326	8.9313	13.468	20.095	21.454
	DQM [31]	3.4339	9.3431	13.912	21.022	21.462
2	Leissa [1]	5.2881	9.6015	19.789	21.603	33.050
	DSC-LK	5.2442	9.4993	19.559	21.374	32.777
	DQEM	5.2782	9.5170	19.596	21.413	32.987
3	Leissa [1]	9.6220	20.735	24.432	46.454	60.137
	DSC-LK	9.5143	20.503	24.212	46.133	59.465
	DQEM	9.5406	20.598	24.270	46.347	59.629
4	Leissa [1]	11.437	22.353	35.024	50.293	71.484
	DSC-LK	11.256	22.125	34.646	49.781	70.349
	DQEM	11.328	22.182	34.801	49.910	70.802
5	Leissa [1]	18.793	25.867	35.024	58.201	117.45
	DSC-LK	18.558	25.564	34.646	57.518	115.98
	DQEM	18.627	25.650	34.801	57.714	116.42
6	Leissa [1]	19.100	29.973	61.526	67.494	119.38
	DSC-LK	18.803	29.648	60.878	66.708	117.52
	DQEM	18.923	29.791	61.093	67.029	118.23

Leissa [1], since Leissa's data are the upper bound solutions. From Tables 7 and 8, it is seen that the accuracy of the present method for the free boundary condition is similar to the matched interface and boundary (MIB) method. From Tables 7–9, it is also observed that the results in [12,31] are not always smaller or larger than Leissa's data [1], some of the data are smaller than Leissa's data, while others are larger than Leissa's data. This phenomenon is obviously caused by the way of applying the boundary conditions. However, the results by DSC-LK and DQEM are consistently smaller than the corresponding Leissa's data, which are the upper bond results. Since $N_x = N_y = 33$ are used in applying the DQEM for comparison purpose, the DQEM results are believed to be the most accurate results presented in Tables 7–9 [30], thus are a little smaller than Lessa's data. The DSC-LK data are a little smaller than the DQEM results.

To well demonstrate the applicability of the proposed method further, five aspect ratios are considered for the FFFF rectangular plate. From Table 9, it is seen by comparing the data with Leissa's data and DQEM results that there is no much difference in the accuracy of DSC-LK data for all five aspect ratios. Based on the results reported herein, one may conclude that the proposed method for applying the free boundary is simple and convenient to use, and can yield reasonable accurate results, although the accuracy of the results is not as high as in the cases of plates without a free boundary.

5. Conclusions

In this paper, free vibration of beams, annular plates and rectangular plates with free boundaries are analyzed by the discrete singular convolution. A simple method to apply the free boundary conditions is proposed. Detailed derivations are given. Eight examples, namely, free vibration of F–C, F–S and F–F beams, F–C and F–S annular plates, and CCCC, CFCC, and FFFF rectangular plates, are analyzed by the DSC. Two kernels, the regularized Shannon's kernel and the non-regularized Lagrange's delta sequence kernel, are tested. It is seen that there is no much difference between frequencies obtained by the DSC with the two kernels for the lower order modes. Results also agree well with existing analytical and numerical solutions and recalculated data by the differential quadrature (element) method.

Based on the results reported herein, one may conclude that the proposed method to incorporate the free boundary conditions, although is simple to use, can yield reasonable accurate frequency data for beams and plates. The DSC's advantages, i.e., the accuracy of global methods and the flexibility of local methods, and accuracy for obtaining the

higher-order modes, seem retained. Thus, the proposed method for applying the boundary conditions extends the application range of the DSC.

Acknowledgement

The work is partially supported by the National Natural Science Foundation of China (10972105).

References

[1] A.W. Leissa, The free vibration of rectangular plates, *Journal of Sound and Vibration* 31 (3) (1973) 257–293.
[2] G.W. Wei, Discrete singular convolution for the solution of the Fokker–Planck equations, *Journal of Chemical Physics* 110 (1999) 8930–8942.
[3] C.H.W. Ng, Y.B. Zhao, G.W. Wei, Comparison of discrete singular convolution and generalized differential quadrature for the vibration of analysis of rectangular plates, *Computer Methods in Applied Mechanics and Engineering* 193 (2004) 2483–2506.
[4] G.W. Wei, Wavelets generated by using discrete singular convolution kernels, *Journal of Physics A: Mathematical and General* 33 (2000) 8577–8596.
[5] G.W. Wei, Y.B. Zhao, Y. Xiang, The determination of natural frequencies of rectangular plates with mixed boundary conditions by discrete singular convolution, *International Journal of Mechanical Sciences* 43 (2001) 1731–1746.
[6] G.W. Wei, A new algorithm for solving some mechanical problems, *Computer Methods in Applied Mechanics and Engineering* 190 (2001) 2017–2030.
[7] G.W. Wei, Discrete singular convolution for beam analysis, *Engineering Structures* 23 (2001) 1045–1053.
[8] Y.B. Zhao, G.W. Wei, DSC analysis of rectangular plates with non-uniform boundary conditions, *Journal of Sound and Vibration* 255 (2) (2005) 203–238.
[9] Y.S. Hou, G.W. Wei, Y. Xiang, DSC-Ritz method for the vibration analysis of Mindlin plates, *International Journal for Numerical Methods in Engineering* 62 (2005) 262–288.
[10] Y.B. Zhao, G.W. Wei, Y. Xiang, Plate vibration under irregular internal supports, *International Journal of Solids and Structures* 39 (2002) 1361–1383.
[11] S. Zhao, G.W. Wei, Y. Xiang, DSC analysis of free-edged beams by an iteratively matched boundary method, *Journal of Sound and Vibration* 284 (2005) 487–493.
[12] S.N. Yu, Y. Xiang, G.W. Wei, Matched interface and boundary (MIB) method for the vibration analysis of plates, Communications in Numerical Methods in Engineering 25 (2009) 923–950.
[13] G.W. Wei, Y.B. Zhao, Y. Xiang, A novel approach for the analysis of high-frequency vibrations, *Journal of Sound and Vibration* 257 (2) (2002) 207–246.
[14] Y.B. Zhao, G.W. Wei, Y. Xiang, Discrete singular convolution for the prediction of high frequency vibration of plates, *International Journal of Solids and Structures* 39 (2002) 65–88.
[15] C.W. Lim, Z.R. Li, G.W. Wei, DSC-Ritz method for the high frequency mode analysis of thick shallow shells, *International Journal for Numerical Methods in Engineering* 62 (2005) 205–232.
[16] Ö. Civalek, Frequency analysis of isotropic conical shells by discrete singular convolution (DSC), *International Journal of Structural Engineering and Mechanics* 25 (1) (2007) 127–131.
[17] Ö. Civalek, Nonlinear analysis of thin rectangular plates on Winkler–Pasternak elastic foundations by DSC–HDQ methods, *Applied Mathematical Modeling* 31 (2007) 606–624.
[18] Ö. Civalek, Numerical analysis of free vibrations of laminated composite conical and cylindrical shells: discrete singular convolution (DSC) approach, *Journal of Computational and Applied Mathematics* 205 (2007) 251–271.
[19] Ö. Civalek, Three-dimensional vibration, buckling and bending analyses of thick rectangular plates based on discrete singular convolution method, *International Journal of Mechanical Sciences* 49 (2007) 752–765.
[20] A. Secgin, A.S. Sarıgu, A novel scheme for the discrete prediction of high-frequency vibration response: discrete singular convolution-mode superposition approach, *Journal of Sound and Vibration* 320 (2009) 1004–1022.
[21] B. He, X. Wang, Error analysis in differential quadrature method, *Transactions of Nanjing University of Aeronautics & Astronautics* 11 (2) (1994) 194–200.
[22] X. Wang, F. Liu, X.F. Wang, et al., New approaches in application of differential quadrature method for fourth-order differential equations, *Communications in Numerical Methods in Engineering* 21 (2) (2005) 61–71.
[23] X. Wang, Y.L. Wang, Y. Zhou, Application of a new differential quadrature element method for free vibrational analysis of beams and frame structures, *Journal of Sound and Vibration* 269 (2004) 1133–1141.
[24] S. Xu, X. Wang, Stress analysis of rectangular plates with sine-distributed loads on two opposite edges by the discrete singular convolution, unpublished manuscript.
[25] A.W. Leissa, *Vibration of Plates (NASA SP 160)*, US Government Printing Office, Washington, DC, 1969.
[26] H.A. Larrondo, V. Topalian, D.R. Avalos, P.A.A. Laura, Comments on "Free vibration analysis of annular plates by the DQ method", *Journal of Sound and Vibration* 177 (1994) 137–139.
[27] D.R. Avalos, H.A. Larrondo, V. Sonzogni, P.A.A. Laura, General approximate solution of the problem of free vibrations of annular plates of non-uniform thickness, Institute of Applied Mechanics, Bahi Bianca, Argentina, Publication No. 96-7, 1995.
[28] X. Wang, A.G. Striz, C.W. Bert, Free vibration analysis of annular plates by the DQ method, *Journal of Sound and Vibration* 164 (1993) 173–175.
[29] X. Wang, Y. Wang, Re-analysis of free vibration of annular plates by the new version of differential quadrature method, *Journal of Sound and Vibration* 278 (2004) 685–689.
[30] Y. Wang, X. Wang, Y. Zhou, Static and free vibration analyses of rectangular plates by the new version of differential quadrature element method, *International Journal for Numerical Methods in Engineering* 59 (2004) 1207–1226.
[31] M. Malik, C.W. Bert, Implementing multiple boundary conditions in the DQ solution of higher-order PDE's: application to free vibration of plates, *International Journal for Numerical Methods in Engineering* 39 (1996) 1237–1258.